Techniques for Efficient Spectrum Sensing in Heterogeneous Wireless Networks

Maurizio Magarini · Luca Reggiani · Arnaldo Spalvieri

Received: date / Accepted: date

Abstract Spectrum sensing is one of the most challenging and complex task in cognitive radio and it should be often performed by mobile devices with a limited battery life. So the development of efficient techniques for advanced spectrum sensing in heterogeneous, ad hoc environments, such as those in emergency situations, is of crucial importance. In this context spectrum sensing can be completed by the determination of the spatial coordinates of the devices in order to achieve the full potential of ad hoc networks management. In this work we present two techniques for improving the efficiency of mobile devices involved in spatial spectrum sensing: design of efficacious frequency synthesizers and hybrid localization for saving energy in the tracking process. Among the different frequency synthesis techniques, we focus on the phase-locked loop (PLL) approach and we consider the optimization of the loop filter for the PLL in the light of Wiener theory by taking into account the phase noise affecting the incoming carrier, the additive white Gaussian noise and the self-noise produced by the phase detector. Then we show an approach for improving the trade-off between energy consumption and performance in a localization tracking process, realized mixing active signal transmissions as well as passive signal reflections.

Keywords spectrum sensing · phase-locked loops (PLLs) · phase noise · localization

M. Magarini, L. Reggiani, A. Spalvieri
Dipartimento di Elettronica e Informazione
Politecnico di Milano
20133 Milano, Italy
Tel.: +39-02-2399-3450
Fax: +39-02-2399-3413
E-mail: {magarini,reggiani,spalvier}@elet.polimi.it

1 Introduction

Easy set-up and rapid deployment of lightweight communication infrastructures are issues of crucial importance for the management of an emergency in disaster areas. In such scenarios, the integration of heterogeneous terrestrial mobile radio networks and their interoperability is required in order to have a telecommunication infrastructure that can rapidly be deployed on the crisis site. The infrastructure is intended to cover immediate needs in the first hours and days after a disaster event, as well as medium to longer term needs, during the recovery and rebuilding phase following an emergency [1].
One of the most critical problems to be addressed in such a networks is represented by the congestion of the frequency spectrum that may occur as the number of participating emergency personnel trying to establish communication with each other increases. Without a proper frequency management system, there is the possibility that different rescue-teams are configured to share the same frequency band. This would result in mutual interference among devices that, as a worst possible case, can lead to the complete loss of communication even among members of the same team. In such circumstances proper spectrum management techniques for radio monitoring and direction-finding are required for rapid discovery of radio interference. Moreover, in these environments the frequency information derived by spectrum sensing should be completed by its spatial coordinates in order to achieve a complete channel state information for the spectrum management in a mobile scenario.
So the identification of free and unused frequency bands as well as the location and tracking of first responders in and around the crisis area become a key issue. Spectrum sensing is one of the most challenging and complex task in cognitive radios where the frequency scanning ranges from tens of megahertz to about 10 GHz [2,3]. Spectrum sensing may also play a crucial role to detect the presence of unknown transmitters in a given area. Channel-by-channel sensing is based on the use of frequency synthesizers whose role is that of providing all necessary frequencies for the down and up conversion with proper channel spacing according to the considered communication standard. Moreover, the local frequency synthesizer has to fulfil the tightest signal purity requirements which can be expressed in terms of the phase noise and the spurious output. Different requirements are specified for different generations of mobile networks such as GSM, UMTS, Bluetooth, WiFi and Mobile WiMAX [4]. The most stringent requirements in terms of phase noise for the local oscillator are imposed by the GSM standard where a Gaussian minimum shift keying (GMSK) modulation is used.
Various approaches for multi-standard frequency synthesizers have been proposed in [5,6]. Although there are many techniques for frequency synthesis, the dominant technique used in wireless technology is based on the phase-lock loop (PLL) principle. This technique is here considered since it offers high performance in terms of the reconfigurability, fine step size and phase noise. As is known, minimum shift keying type (MSK-type) signals can be regarded as approximated forms of offset quadrature phase-shift keying (OQPSK) when

the first term of the Laurent's decomposition dominates the series [7]. This suggests the extension of synchronization algorithms usually employed for OQPSK to MSK-type signals [8]. In the design of the PLL for OQPSK and MSK-type formats it is worth taking into account the self-noise that affects the phase detector, a noise that is not present in quadrature amplitude modulation (QAM) and phase-shift keying (PSK) formats. In Sec. 3 we focus on the design of the loop filter by extending the Wiener's approach, studied in [9] for QAM modulation formats, to the case where self-noise is present, enabling application to OQPSK and MSK-type formats.

Then, in Sec. 4 we present an algorithm for tracking mobile devices that can behave alternatively as active transmitters and passive scatterers or even simple relays [11]. The proposed algorithm is used for saving energy in small mobile devices, or sensors, and it uses only estimates of multi-path propagation delays and no angle-of-arrival information. The possible application areas of this type of algorithm are numerous including ad hoc radio infrastructures for implementing broadband location-based services, such as spectrum sensing in emergency environments. The tracking algorithm described in this work is based on a relatively simple approach since it is realized by mixing active signal transmissions that allow using usual techniques for deriving distances and locations as well as passive signal receptions that exploit diffused reflections caused by the target (as a passive small scattering object or a simple relay) during signal propagation. The tracking algorithm, by means of a bank of Extended Kalman Filters (EKFs), combine these two types of transmissions.

2 System model

The network under consideration is an asynchronous network composed of a fixed number N of mobile devices distributed over a delimited area, and with two-dimensional coordinates (x, y). The network has no centralized medium access control, lacks a global clock reference, and nodes have no a-priori channel state information. In this paper, all nodes transmit packets, randomly offset in time and with a node specific and globally known preamble. Each packet is time-stamped with respect to the local clock at the transmitting node.

At the generic node, the complex envelope of the continuous-time received signal is

$$r(t) = e^{j\theta(t)} \sum_i a_i u(t - iT) + w(t), \tag{1}$$

where j is the imaginary unit, $a_k = \pm 1$ for k even and $a_k = \pm j$ for k odd, $\theta(t)$ is the phase noise, $u(t)$ is the impulse response of the shaping filter, T is the bit repetition interval, and $w(t)$ is the complex additive white Gaussian noise with power spectral density N_0. The model given by equation (1) holds exactly for OQPSK and MSK, while it provides a close approximation for many MSK-type signals of practical interest, as for instance the popular GMSK with $BT = 0.3$, when the impulse response $u(t)$ is the first term of the Laurent decomposition. The received signal is filtered through the matched filter $u^*(-t)$, sampled at

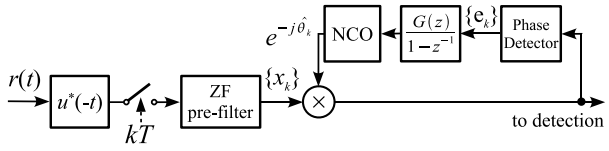

Fig. 1 Block diagram of the system.

the time instants kT and filtered through the zero forcing (ZF) pre-filter with frequency response

$$C(e^{j2\pi fT}) = \frac{2T}{\sum_k |U(f - \frac{k}{2T})|^2},$$

where $U(f)$ is the Fourier transform of $u(t)$. The kth sample of the signal at the output of the pre-filter has the form

$$x_k = e^{j\theta_k} \sum_i a_i v_{k-i} + n_k,$$

where the samples of the impulse response $\{v_k\}$ satisfy the Nyquist condition in the form $v_0 = 1$ and $v_{2k} = 0$, for $k \neq 0$. The sequence $\{n_k\}$ is the complex additive Gaussian noise with power spectral density

$$\Psi_n(e^{j2\pi fT}) = \frac{N_0}{T} |C(e^{j2\pi fT})|^2 | \sum_k U^*(f - \frac{k}{T})|^2.$$

The kth sample at the output of the phase detector is

$$e_k = \Im\{a_k^* x_k e^{-j\hat{\theta}_k}\} = \sin(\theta_k - \hat{\theta}_k) + \lambda_k \cos(\theta_k - \hat{\theta}_k) + \xi_k, \tag{2}$$

where the superscript * denotes complex conjugation, $\Im\{x\}$ extracts the imaginary part of x and $\hat{\theta}_k$ is the kth phase sample produced by the carrier recovery loop. The sequence $\{e_k\}$ is filtered and used to produce the carrier estimate by a number controlled oscillator (NCO). The block diagram of the system is reported in figure 1. The even and the odd samples of the Gaussian noise $\{\xi_k\}$ come from the imaginary and the real part of $\{n_k\}$, respectively, and therefore are uncorrelated. The power spectral density of $\{\xi_k\}$ is

$$\Psi_\xi(e^{j2\pi fT}) = \frac{1}{4}\Psi_n(e^{j2\pi fT}) + \frac{1}{4}\Psi_n(e^{j2\pi(f-\frac{1}{2T})T}),$$

where the factor $1/4$ comes from the folding (factor $1/2$) and from the projection of the complex noise over one dimension (factor $1/2$).
The kth sample of the self-noise is

$$\lambda_k = \sum_i \Im\{a_k^* a_{k-2i-1}\} v_{2i+1}.$$

In what follows we use the z-transform to represent sequences, where z^{-1} is the unit delay, that is, T. The z-spectrum of $\{\lambda_k\}$ is

$$\Psi_\lambda(z) = \sum_i v_{2i+1}^2 - \sum_k v_{2k+1}^2 z^{-2k-1}.$$

Note that the power spectrum of self-noise depends on the odd samples of $\{v_k\}$. When $|\sum_k U^*(f - k/T)|^2$ satisfies the condition of not having spectral zeros, as it happens for instance with GMSK, it is possible to design the pre-filter in such a way that the condition $v_k = \delta_k$ is satisfied (δ_i denotes the Kronecker delta). This design of the pre-filter induces noise enhancement. However, at high signal-to-noise ratio, noise enhancement can be accepted. Also note that, when $U(f)$ is the square root of a Nyquist filter, as it often happens with OQPSK, we obtain

$$\Psi_\xi(z) = \frac{N_0}{2E_b}, \tag{3}$$

where $E_b = \int_{-\infty}^{\infty} |u(t)|^2 dt$ is the energy per bit.

3 Wiener Design of the Loop Filter in Digital PLL-based Frequency Synthesizers

For small phase error the phase detector can be linearized, $\sin(\theta - \hat{\theta}) \approx \theta - \hat{\theta}$, $\cos(\theta - \hat{\theta}) \approx 1$, leading to the error polynomial

$$E(z) = \Theta(z) - \hat{\Theta}(z) + \Lambda(z) + \Xi(z).$$

The *open-loop transfer function* is

$$G(z) = \frac{\hat{\Theta}(z)}{E(z)} = \sum_{k=K}^{\infty} g_k z^{-k},$$

where $K > 0$ is the delay of the loop. The number of poles of $G(z)$ is the *order* of the loop, while the number of poles of $G(z)$ at $z = 1$ is the *type* of the loop. In the analysis of the loop it is useful to introduce the polynomial

$$Y(z) = \Theta(z) + \Lambda(z) + \Xi(z). \tag{4}$$

We assume that $\{\theta_k\}$, $\{\lambda_k\}$ and $\{\xi_k\}$ are independent random sequences, therefore the z-spectrum of $\{y_k\}$ is

$$\Psi_y(z) = \Psi_\theta(z) + \Psi_\lambda(z) + \Psi_\xi(z). \tag{5}$$

The *closed-loop transfer function* is

$$H(z) = \frac{G(z)}{1 + G(z)} = \frac{\hat{\Theta}(z)}{Y(z)}. \tag{6}$$

The optimal $H(z)$ is obtained from the Wiener-Hopf equations. Following the steps of [9] we get

$$H(z) = \alpha^2(1 - P(z))[(1 - P(z^{-1}))\Psi_\theta(z)]_K^\infty, \tag{7}$$

where the notation $[X(z)]_i^j = \sum_{k=i}^{j} x_k z^{-k}$ is used. The real number α^2 is computed by Szego's formula and $1 - P(z)$ is the causal monic and minimum phase transfer function which results from the spectral factorization

$$(1 - P(z))\,\alpha^2\left(1 - P(z^{-1})\right) = \Psi_y^{-1}(z). \tag{8}$$

3.1 Approximate solution

We observe that in many cases of practical interest the bandwidth of the loop filter is small compared to the bit frequency, therefore we aim to approximate the spectrum of self-noise and the spectrum of channel noise in the low frequency region. The spectrum of self-noise is well approximated in the low frequency region by

$$\Psi_\lambda(z) = (1 - z^{-1})\gamma_2(1 - z), \tag{9}$$

with $\gamma_2 = \sum_{k=0}^{\infty}(2k + 1)^2 v_{2k+1}^2$. The spectrum of the additive channel noise $\{\xi_k\}$ is approximated in the low frequency region by (3). Using (3) and (9) in (5) and performing the spectral factorization, we obtain

$$H(z) = \frac{[Q(z) + \alpha^2\gamma_2 z^{-1}]_K^\infty}{1 + Q(z)}, \tag{10}$$

and the mean square error (MSE)

$$E\{(\theta_i - \hat{\theta}_i)^2\} = \frac{1}{\alpha^2} + \sum_{k=1}^{K-1}\frac{q_k^2}{\alpha^2} - 2\gamma_2 - \frac{N_0}{2E_b} - \left(\alpha^2\gamma_2^2 + 2\gamma_2 q_1\right)\delta_{K-1}, \tag{11}$$

where $1 + Q(z) = (1 - P(z))^{-1}$.

3.2 Case study

Assume that the phase noise is the sum of random phase walk plus white phase. The phase noise spectrum is

$$\Psi_\theta(z) = \frac{\gamma_{-2}}{(1 - z^{-1})(1 - z)} + \gamma_0.$$

The spectral factorization is performed by root finding. The result is

$$1 - P(z) = \frac{1 - z^{-1}}{(1 - z_1 z^{-1})(1 - z_2 z^{-1})},$$

$$Q(z) = \frac{(1 - z_1 - z_2)z^{-1}}{1 - z^{-1}}\left(1 + \frac{z_1 z_2}{1 - z_1 - z_2}z^{-1}\right), \tag{12}$$

where the two roots are

$$z_i = \frac{x_i - \sqrt{x_i^2 - 4}}{2}, \quad i = 1, 2,$$

with

$$x_{1,2} = 2 + \frac{\gamma_0 + \frac{N_0}{2E_b}}{2\gamma_2} \pm \sqrt{\left(\frac{\gamma_0 + \frac{N_0}{2E_b}}{2\gamma_2}\right)^2 - \frac{\gamma_{-2}}{\gamma_2}}.$$

Putting (12) in equation (10) and using (6) one gets

$$H(z) = \frac{(1 - z_1 - z_2 + z_1 z_2) z^{-K}}{(1 - z_1 z^{-1})(1 - z_2 z^{-1})}, \tag{13}$$

$$G(z) = \frac{(1 - z_1 - z_2 + z_1 z_2) z^{-K}}{(1 - z^{-1})(1 - z_1 z_2 z^{-1} + \sum_{k=1}^{K-1} (1 - z_1 - z_2 + z_1 z_2) z^{-k})}.$$

Note that with $K = 1$ and without self-noise one would obtain an optimal type-I, order 1 loop [9]. The presence of self-noise has increased the order of the optimal loop inducing a pole at $z = z_1 z_2$. For $K > 1$ a type-I order K loop is obtained. Using (12) and substituting $\alpha^2 = z_1 z_2 / \gamma_2$ in equation (11) we get for the MSE

$$E\{(\theta_i - \hat{\theta}_i)^2\} = \gamma_2 \left(\frac{1}{z_1 z_2} + 2z_1 + 2z_2 - z_1 z_2 - 4\right) + \frac{\gamma_2}{z_1 z_2}(K-1)(1 - z_1 - z_2 + z_1 z_2)^2 - \frac{N_0}{2E_b}. \tag{14}$$

3.3 Numerical Results

Numerical results are derived for GMSK with $BT = 0.3$. The spectrum of phase noise that affects the free-running oscillator used for the analysis is characterized by $\gamma_{-2} = 5 \cdot 10^{-5}$ and $\gamma_0 = 10^{-4}$. Figure 2 shows analytical results and simulation results for the MSE versus $2E_b/N_0$ for $K = 1$ and $K = 32$. Note that, while analytical results have been obtained assuming that no decision errors affect the phase detector (2), in the simulations the phase detector makes use of decisions in place of true data. At low SNR simulation results deviate from the theory due to decision errors. The best MSE is given by the optimum $H(z)$ obtained without approximations using the numeric exp – log method [10]. From the figure we see that the use of the loop filter we propose gives a benefit of about 2 dB on the floor compared to the classical order-I type 1 loop when $K = 1$. When $K > 1$ the benefit diminishes. Also observe that the performance of the approximated transfer function derived in Sect. 3.1 is close to the optimal one.

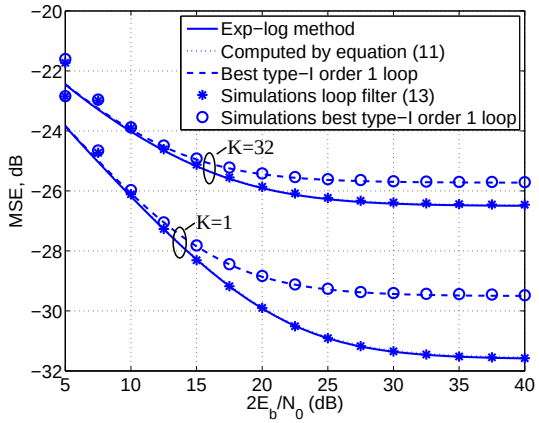

Fig. 2 MSE versus $2E_b/N_0$ for GMSK with $BT = 0.3$.

4 Device localization

According to the wireless network briefly described in Sect. 2, the N nodes can cooperatively estimate their unknown positions by means of standard localization and tracking techniques based on the times of arrival of the received packets [13].

The principle presented here is simple: the target device alternates phases in which it acts as an active transmitter with signal regeneration (namely it transmit a specific packet to the beacons for allowing estimation of times of arrival and distances as in Fig. 3-a) to phases without signal regeneration in which it acts as a passive scatterer or a simple relay (Fig. 3-b). The difference between these two phases at the beacons is the following: in regenerative phases the beacons exploit the signal received from the target for estimating the corresponding distance while, in the non-regenerative phases, the beacons derive measures on the total reflected paths between each couple of beacons (Fig. 3). The necessity of using reflected paths between two beacons and not direct reflected paths (e.g. between each beacon and the target) relies on the fact that each node could not be able to transmit and receive simultaneously. From the target perspective, regenerative and non-regenerative phases differ in the energy consumption and this aspect can be interesting in a series of applications where small, inexpensive devices should benefit from energy savings also at the expense of possibly limited performance reductions. The localization algorithm incorporates two key components described in the next Sect. 4.1 and 4.2: ranging in regenerative and non-regenerative phases and tracking, operated by a bank of EKFs.

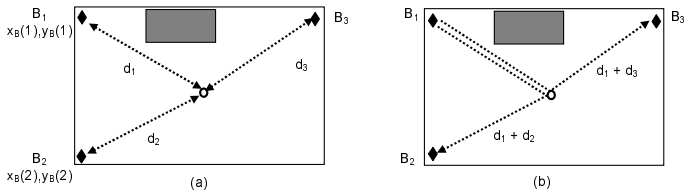

Fig. 3 Combination of regenerative (a) and non-regenerative (b) measures.

4.1 Ranging

We only give a brief overview of the ranging algorithms used in this work, and refer to [14], and references cited therein, for additional details. When the target is in a regenerative phase, the i-th beacon estimates the direct distance d_i to the target. On the other hand, when the target is in a non-regenerative phase, each couple of beacons, i and j, is interested by the measure of the reflected or relayed path, $d_i + d_j$ (Fig. 3).
In this work we use two different ranging algorithms. The former is a low-complexity estimator based on a threshold for detecting the first path [15], while the latter outputs a discrete vector of likely distances with an associated approximation of the probability that these distances correspond to the estimates [14]. This soft information is also used to provide a measure of the uncertainty of the distance estimate, i.e., an estimate of the error magnitude; in fact a large uncertainty is often associated to a NLOS measure or to a measure obtained at low Signal-to-Noise Ratio (SNR). In this case, note that detection of a path cluster arrival is performed on the difference between the signal received at the j-th beacon and the signal corresponding to the environment without the target (stored at each beacon before the insertion of any target); this step is necessary for estimating the time of arrivals only on the new paths, generated by the target.

4.2 Tracking

The tracking system is based on one or on a bank of N_{EKF} EKFs [16]. At k-th step, the state $\mathbf{x}$ of each EKF is represented by a vector containing the current location, velocity and acceleration of the target in bi-dimensional coordinates, i.e. $\mathbf{x} = \{x_k, y_k, v_{x,k}, v_{y,k}, a_{x,k}, a_{y,k}\}$. This set of multiple filters is necessary when tracking more targets or/and when managing multiple measures and likelihoods associated to a single target; in this latter case a metric is built and updated for selecting the most likely trajectories in a hypothesis tree that is updated at each step of the tracking process. We have considered two different strategies in order to exploit the information provided by the soft multi-path distance estimator. The first approach, EKF with dynamic measure variance update (EKF-DMVU), is mainly intended for a single object tracking and it uses the likelihood vectors for computing local estimates of

the instantaneous error variance of the multi-path distance measurements; the rationale behind this approach is that if some channel estimate has more than one component with a significant probability, then the corresponding distance estimate can be considered more uncertain, and vice versa. In the second approach, referred as Multiple Hypotheses EKF (MH-EKF), the N_{EKF} parallel EKFs are used to track one or more moving objects. In the filter bank, each EKF must, at each measurement cycle, select one estimate from each beacons pair (in a non-regenerative phase) or from one beacon-target link (in a regenerative phase) in a possibly large number of different estimates with varying likelihood values. Each EKF in the filter bank has an associated figure of merit, which measures how well the filter has tracked its intended target until k-th step in the hypothesis tree. More details about the application of these algorithms and their variants can be found in [12]. Here, the innovative part of this method is constituted by mixing the distance measures provided by the regenerative and non-regenerative phases (or steps in the tracking process). This mixing responds to a pre-defined pattern characterized by the fraction λ of non-regenerative steps w.r.t. the total one; so the generic pattern has a period composed by N_{REG} regenerative and $(1-\lambda)/\lambda \cdot N_{REG}$ non-regenerative steps. Energy savings will be proportional to the factor λ.
In Fig. 4 we report an example of performance obtained for a single target moving along random trajectories in a square area of 30 m in a network composed by other 4 fixed nodes at the area corners. In all the scenarios, numerical findings, which are expressed by the root mean squared error (RMSE) for a wide spectrum of the factor λ, show the advantage provided by the use of more sophisticated soft ranging algorithm w.r.t. the threshold version (Sec. 4.1) and the further gain obtained by exploiting an hypothesis tree with a bank of at least 2 EKFs. It is also interesting to note how performance is also less sensitive to the factor λ for the most advanced localization solutions, opening the possibility of advantageous trade-offs between energy savings and performance.

5 Conclusions

The main novel results of this work are (i) the optimal loop filter and MSE for carrier recovery based on discrete-time PLL for MSK-type modulation formats and (ii) a simple principle for tuning a trade-off between energy consumption and localization performance. Both these techniques can be exploited for increasing performance and efficiency of spatial spectrum sensing in ad hoc mobile networks.

References

1. F. Chiti, R. Fantacci, L. Maccari, D. Marabissi, and D. Tarchi, “A broadband wireless communications system for emergency management,” IEEE Wireless Communications Magazine, pp. 8-14, (2008).

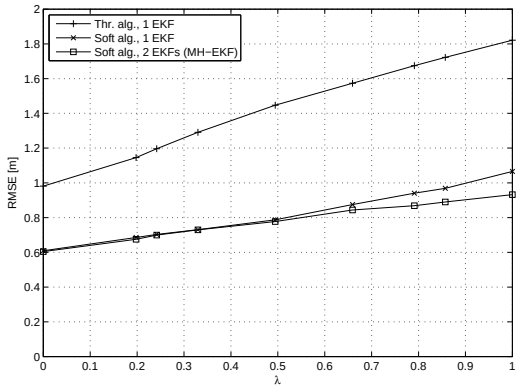

Fig. 4 Root mean square location error for a square area with side $d = 30$ m.

2. B. Razavi, "Challenges in the Design of Cognitive Radios," in Proc. Custom Intergrated Circuits Conf. (CICC), pp. 391-398 (2009).
3. A. Haniz, M. A. Rahman, M. Kim, and J. Takada, "Spectrum sensing on emergency radio spectrum management system," in Proc. Int. Symp. on Commun. and Inform. Technol. (ISCIT), pp. 985-990 (2010).
4. V. Valenta, G. Baudoin, and M. Villegas, "Phase noise analysis of PLL based frequency synthesizers for multi-radio mobile terminals," in Proc. Int. Conf. on Cognitive Radio Oriented Wireless Networks and Commun. (CROWNCOM), pp. 1-4 (2008).
5. A. Koukab, Y. Lei, J. Declercq, "A GSM-GPRS/UMTS FDD-TDD/WLAN 802.11a-b-g multi-standard carrier generation system, IEEE J. Solid-State Circuits, Vol. 41, pp. 1513-1521 (2006).
6. I. L. Syllaios, P. T. Balsara, R. B. Staszewski, "On the reconfigurability of all-digital phase-locked loops for software defined radios, in Proc. Int. Symp. Personal, Indoor and Mobile Radio Commun. (PIMRC), pp. 1-6 (2007).
7. P. A. Laurent,"Exact and approximate construction of digital phase modulatins by superposition of amplitude modulated signals," *IEEE Trans. Commun.*, Vol. 34, pp. 150-160 (1986).
8. U. Mengali and A. N. D'Andrea, Synchronization Techniques for Digital Receivers. Plenum Press, New York (1997).
9. A. Spalvieri, M. Magarini, "Wiener's analysis of the discrete-time phase-locked loop with loop delay," IEEE Trans. Circuits Syst. II, Exp. Briefs, Vol. 55, pp. 596-600 (2008).
10. M. H. Hayes, *Statistical Digital Signal Processing and Modeling*. New York: Wiley, 1996, § 3.5.
11. L. Reggiani, R. Morichetti, "Hybrid active and passive localization for small targets," 2010 International Conference on Indoor Positioning and Indoor Navigation (IPIN), pp.1-5, Sept. 2010.
12. L. Reggiani, M. Rydstrom, G. Tiberi, E. G. Strom, and A. Monorchio, "Ultra-wide band sensor networks for tracking point scatterers or relays," in *Proc. IEEE ISWCS*, 2009.
13. I. Guvenc, Chia-Chin Chong, "A Survey on TOA Based Wireless Localization and NLOS Mitigation Techniques," IEEE Communications Surveys and Tutorials, vol.11, no.3, pp.107-124, 3rd Quarter 2009.
14. M. Rydström, L. Reggiani, E. G. Ström, and A. Svensson, "Sub-optimal soft range estimators with applications in UWB sensor networks," *IEEE Transactions on Signal Processing*, vol. 56, pp. 4856–4866, 2008.
15. J.-Y. Lee and R. A. Scholtz, "Problems in modeling UWB channels," *Proc. Asilomar Conf. on Systems and Computers*, vol. 1, pp. 706–711, 2002.
16. S. Haykin, *Adaptive filter theory*, 4th ed. Prentice Hall, 2002.